Supplementary material

MicroRNA-26a-3p rescues depression-like behaviors in male rats via preventing hippocampal neuronal anomalies

Ye Li [1], Cuiqin Fan[1], Liyan Wang[2], Tian Lan[1], Rui Gao[3], Wenjing Wang[1], Shu Yan Yu[1, 4] *

Supplementary Methods and Materials

Open field test (OPT)

The open field test was used to measure the spontaneous locomotor activity as described previously (Walsh and Cummins 1976). Rats were individually placed in the center of a square box (100 x 100 x 40 cm) and were permitted unrestricted move throughout the arena for a 5-min session. The number of locomotor (segments crossed with the four limbs) and exploratory activities (number of rearings, consisting of standing on their hind limbs) were recorded by the observer blind to the treatment group.

Novel object recognition task

The novel object recognition (NOR) task was used to test the non-spatial short-term memory as described previously (Ennaceur and Delacour 1988). Briefly, rats were individually placed in the empty chamber (60 x 40 x 40 cm) for a 1h habituation. On the next day, each rat was placed in the same chamber for a 10 min re-habituation period and then was placed in the chamber with two identical objects for 3min. After a 1 h interval, the rat was returned to the chamber with one of the object was replaced with a novel object for 3min test. Exploratory behavior was defined as sniffing, touching and moving vibrissae whilst directing the nose towards the object within the distance of 1 cm. The discrimination ratio of the novel from familiar object was presented as: novel/ (novel + familiar time).

Supplementary Figure 1

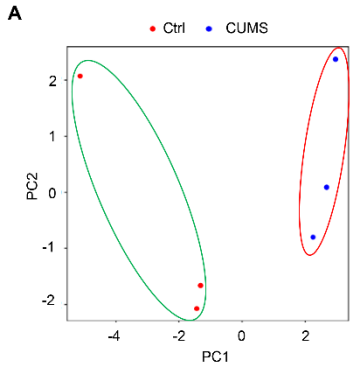

Supplementary Figure 1. The principal component analysis (PCA) plot showed the reproducibility of the RNA-seq experiments.

Supplementary Figure 2

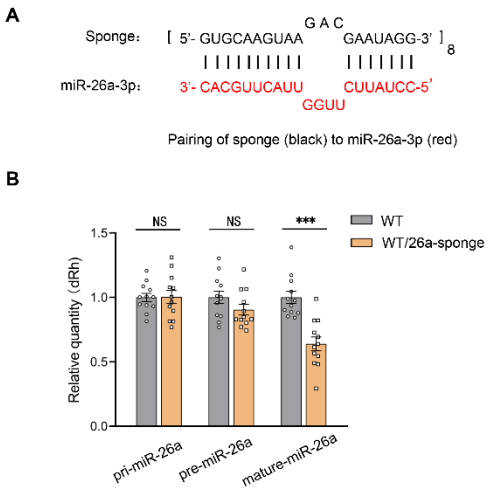

Supplementary Figure 2. The miR-26a-sponge binds to the target miRNA through imperfect complementarity. (A) The complementation between the sequence of sponge and miR-26a-3p shows that the sponge contains multiple imperfect miRNA binding sites. The sequence of miRNA sponge construct is: 5' GUGCAAGUAAGACGAAUAGG 3'. The scramble sequence of the control construct for the miR-26a-sponge is: 5' GCUUCCGUCAUUUCAAUCUGU 3'. **(B)** Quantitative real-time PCR showed that the expression levels of pri-miR-26a and pre-miR-26a in DG regions have no changes after injection of AAV-miR-26a-sponge in DG region. N=12 rats per group from 3 independent biological replicate experiments. *P< 0.05, **P<0.01, ***P<0.001 when compared to the WT group. Data were analyzed with Student's t test. WT, wide type.

Supplementary Figure 3

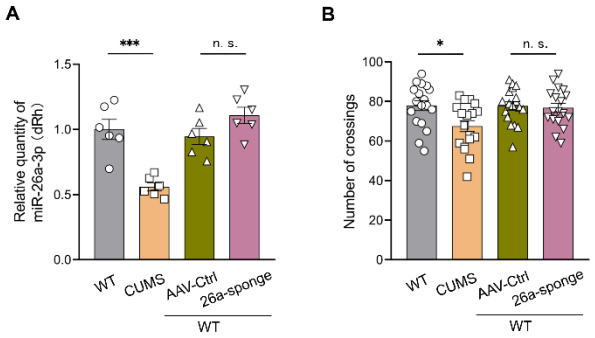

Supplementary Figure 3. The effects of knock-down of miR-26a-3p within the DG on the locomotor behaviors in normal rats. (**A**) Quantitative real-time PCR showed that the expression levels of miR-26a-3p in CA1 regions have no changes after injection of AAV-miR-26a-sponge in DG region. N=6 rats per group from 3 independent biological replicate experiments. **(B)** Knock-down of miR-26a-3p within the DG of normal rats has no effects on the locomotor behaviors in rats. Each column represents the mean ± SEM from 16 to 18 animals per group. *p < 0.05, **P<0.01, ***P<0.001 when compared to the normal control, n.s. when compared to the AAV-control rats. Data were analyzed with a one-way ANOVA, followed by the Tukey's correction. WT, wide type; Ctrl, control.

Supplementary Figure 4

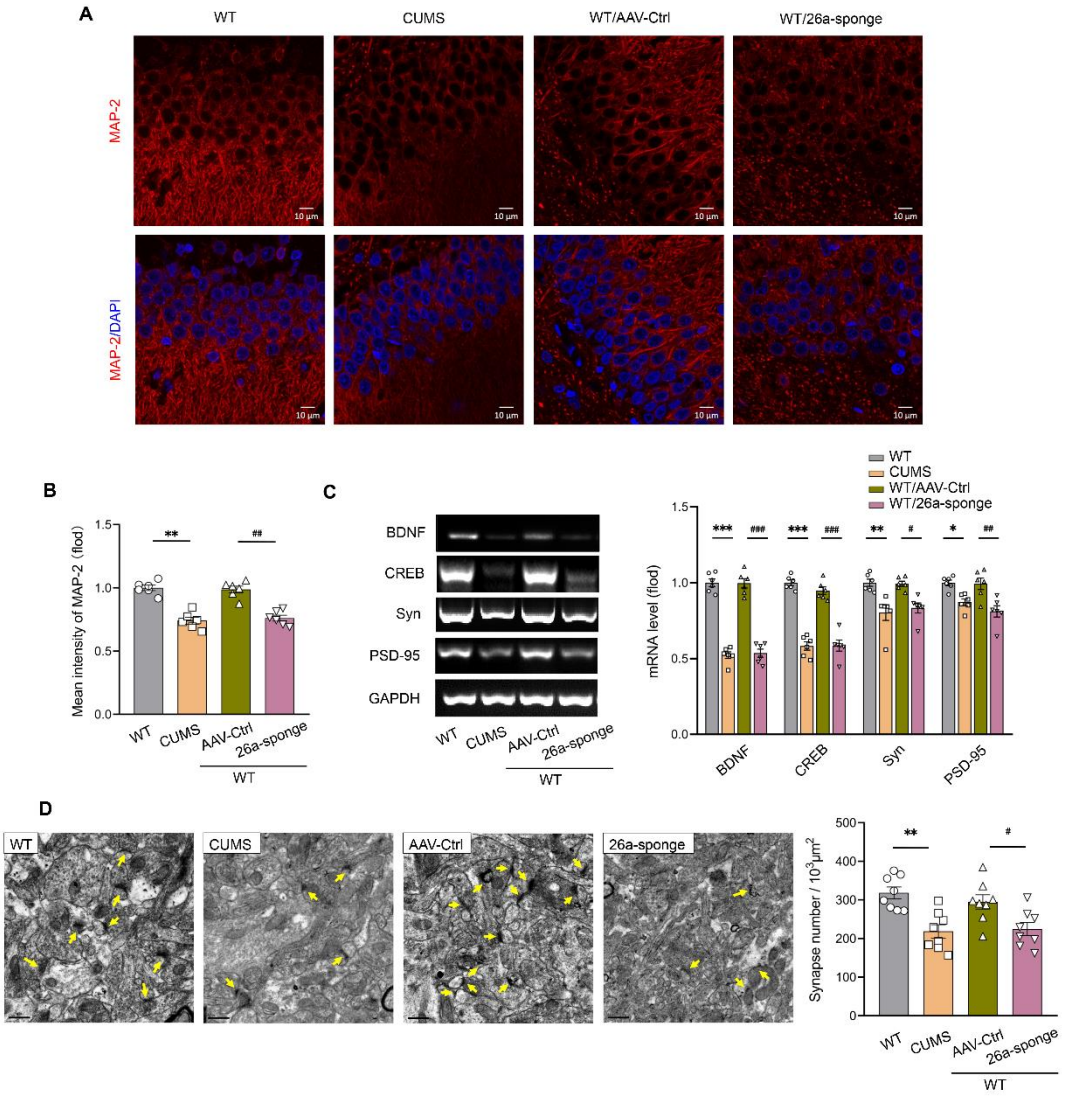

Supplementary Figure 4. Knock-down of miR-26a-3p within the DG of normal rats induced dysregulation of neuroplasticity. (**A**, **B**) Representative confocal microscopic images showing expressions of MAP-2 within the DG of different groups. Scale bar = 10μm. N=6 rats per group and at least 4-6 images from 1 animal. (**C**) Knock-down of miR-26a-3p decreased mRNA levels of neuroplasticity-related mediators in the DG. N=6 rats per group from 3 independent biological replicate experiments. (D) Representative electronic micrographs and summary of data showing synapse densities

within the DG of different groups. Scale bar = 500nm. N = 8 rats per group and at least 20 micrographs from 1 animal. electron microscope and immunofluorescence were repeated at least 3 times and quantitation was done for representative samples from each group. Data are presented as the means ± SEM. *P<0.05, **P<0.01, ***P<0.001 vs. WT; $^{\#}$P<0.05, $^{\#\#}$P<0.01, $^{\#\#\#}$P<0.01vs. AAV-control (WT+ AAV-control) by ANOVA with Tukey's post hoc correction. WT, wide type; Ctrl, control.

Supplementary Figure 5

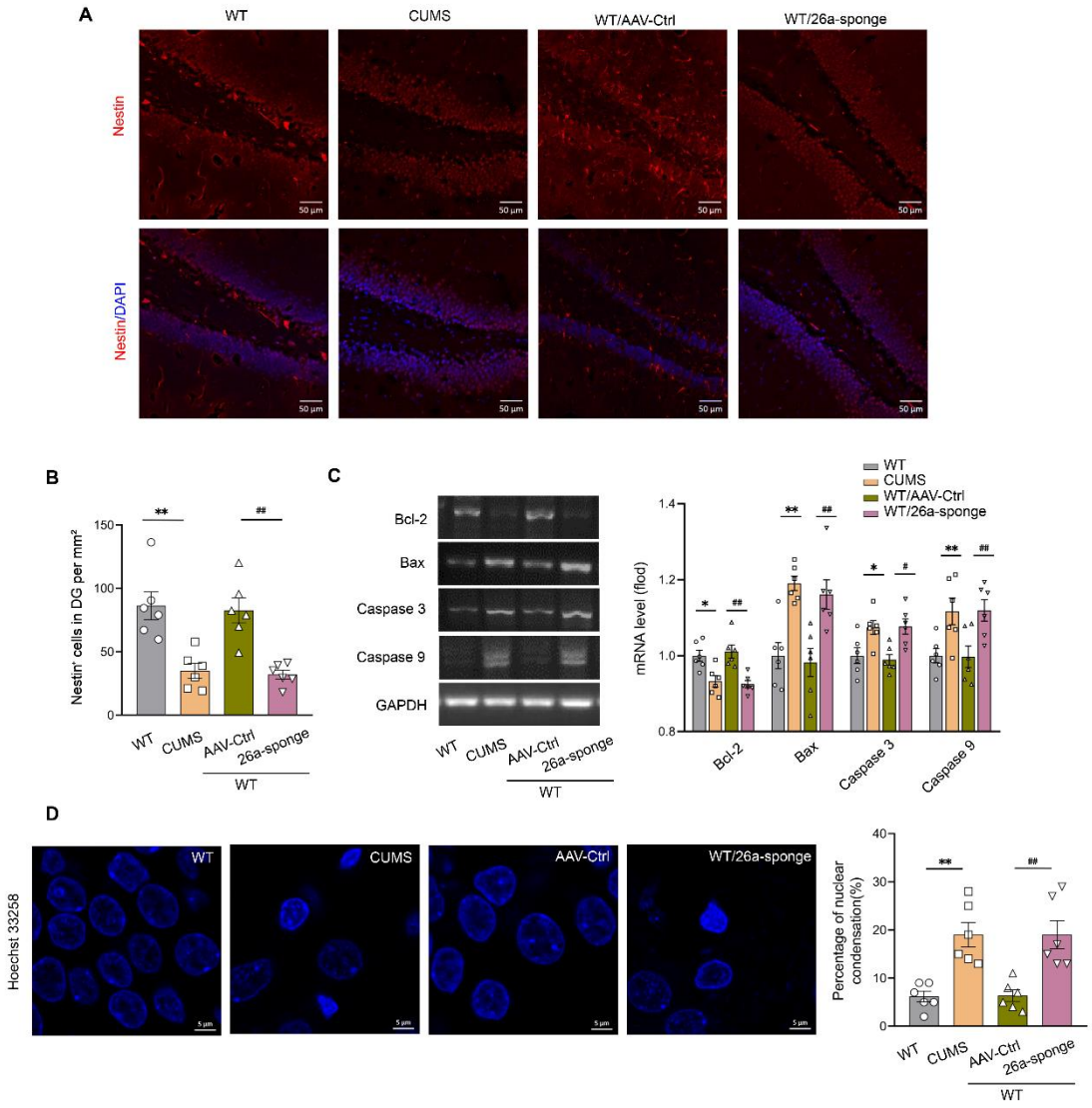

Supplementary Figure 5. Knock-down of miR-26a-3p within the DG of normal rats induced neuronal apoptosis. (A, B) Representative confocal microscopic images showing expressions of Nestin within the DG of different groups. Scale bar = 10μm. N=6 rats per group and at least 4-6 images from 1 animal. (C) Knock-down of miR-26a-3p increased mRNA levels of pro-apoptotic factors in the DG. N=6 rats per group from 3 independent biological replicate experiments. (D) Representative Hoechst images of 33258 staining and summary of data showing nuclear staining in the DG of

different groups. Scale bar = 5μm. N = 6 rats per group and at least 4-6 images from 1 animal. Immunofluorescence were repeated at least 3 times and quantitation was done for representative samples from each group. Data are presented as the means ± SEM. *P<0.05, **P<0.01 vs. WT; $^{\#}$P<0.05, $^{\#\#}$P<0.01 vs. AAV-control (WT+ AAV-control) by ANOVA with Tukey post hoc correction. WT, wide type; Ctrl, control.

Supplementary Figure 6

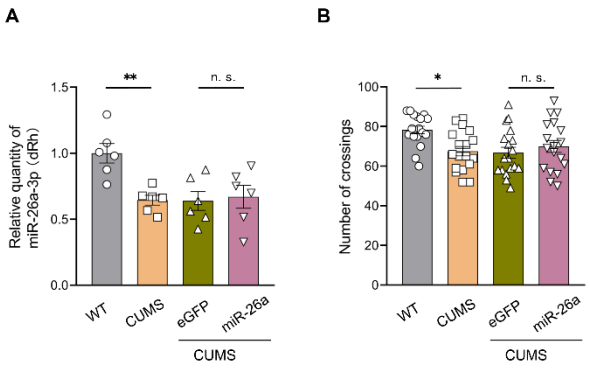

Supplementary Figure 6. Overexpression of miR-26a-3p in the DG of CUMS rat on has no effects on the locomotor behaviors of rats. (**A**) Quantitative real-time PCR showed that the expression levels of miR-26a-3p in CA1 regions have no changes after injection of AAV-miR-26a-sponge in DG region. N=6 rats per group from 3 independent biological replicate experiments. (**B**) Overexpression of miR-26a-3p within the DG of CUMS rats has no effects on the locomotor behaviors in rats. Data are presented as the means ± SEM. Each column represents the mean ± SEM from 16 to 18 animals per group. *P<0.05, **P<0.01 vs. WT; n.s. vs. eGFP control (CUMS+ AAV-eGFP) by ANOVA with Tukey post hoc correction. WT, wide type.

Supplementary Figure 7

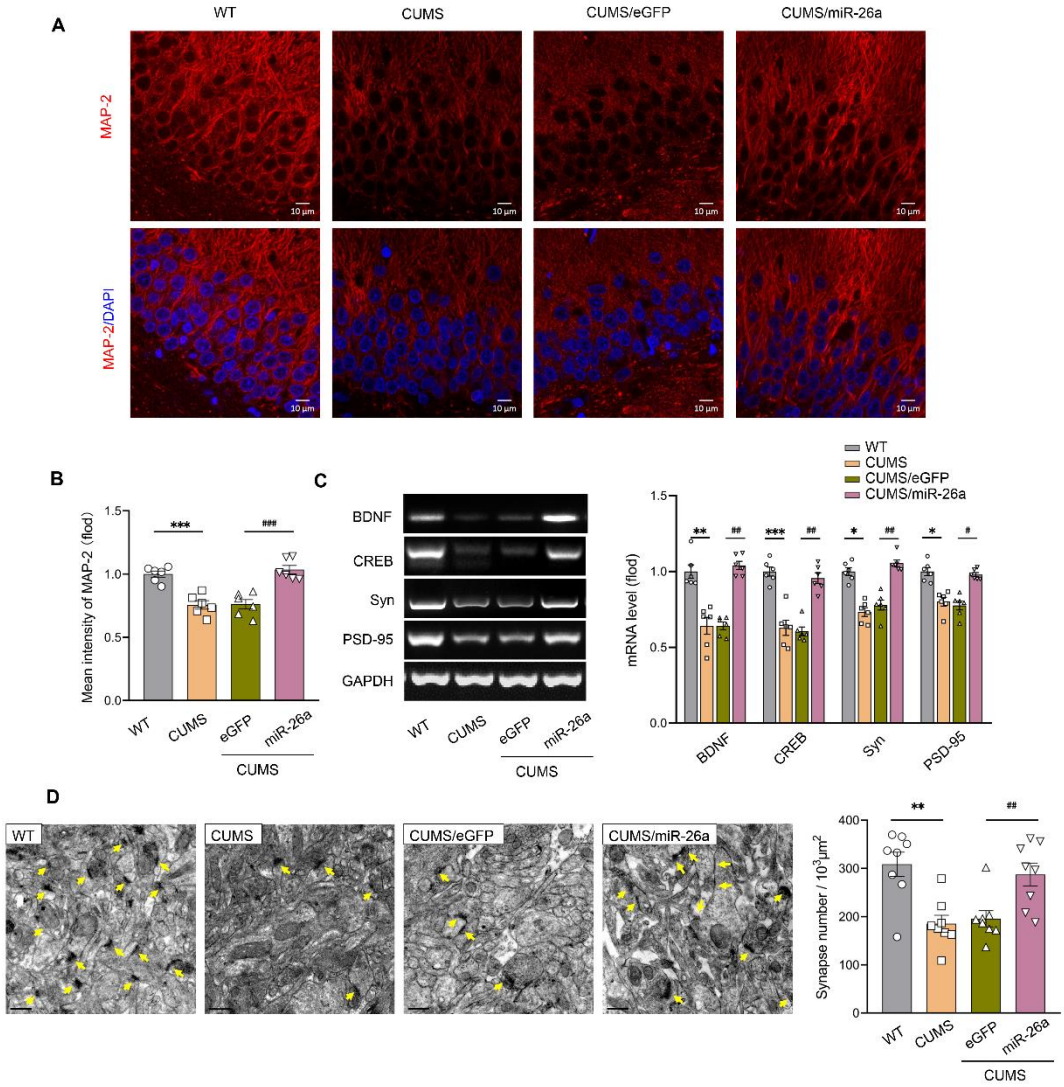

Supplementary Figure 7. Overexpression of miR-26a-3p in the DG of CUMS rats restored the dysregulation of neuroplasticity resulting from CUMS exposure. (**A, B**) Representative confocal microscopic images showing the expression levels of MAP-2 within the DG. Scale bar = 10μm. N=6 rats per group and at least 4-6 images from 1 animal. (**C**) Overexpression of miR-26a-3p increased mRNA levels of neuroplasticity-related mediators in CUMS rats. N=6 rats per group from 3 independent biological replicate experiments. (D) Representative electronic micrographs and summary of data

showing synapse densities within the DG. Scale bar = 500 nm. N = 8 rats per group and at least 20 micrographs from 1 animal. Electron microscope and immunofluorescence were repeated at least 3 times and quantitation was done for representative samples from each group. Data are presented as the means ± SEM. *P<0.05, **P<0.01, ***P<0.001 vs. WT; $^{\#}$P<0.05, $^{\#\#}$P<0.01, $^{\#\#\#}$P<0.001 vs. eGFP control (CUMS+ AAV-eGFP) by ANOVA with Tukey post hoc correction. WT, wide type.

Supplementary Figure 8

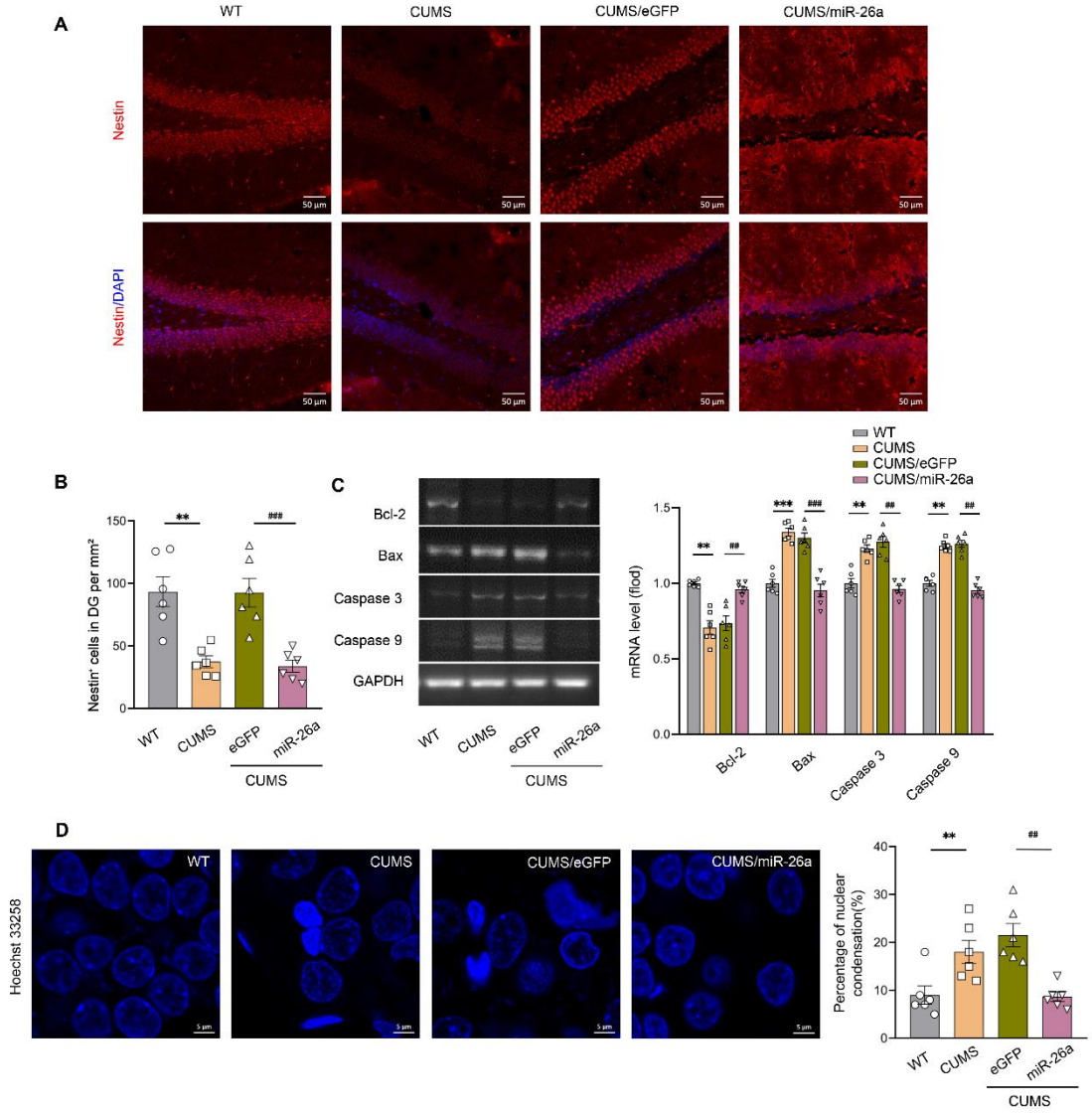

Supplementary Figure 8. Overexpression of miR-26a-3p within the DG of CUMS rats suppressed neuronal apoptosis resulting from CUMS exposure. (A, B) Representative confocal microscopic images showing expressions of nestin within the DG. Scale bar = 50μm. N=6 rats per group and at least 4-6 images from 1 animal. (C) Overexpression of miR-26a-3p decreased mRNA levels of apoptosis-related factors in CUMS rats. N=6 rats per group from 3 independent biological replicate experiments. (D) Representative images of Hoechst 33258 staining and summary of data showing

nuclear staining in the DG. Scale bar = 5μm. N = 6 rats per group and at least 4-6 images from 1 animal. Immunofluorescence were repeated at least 3 times and quantitation was done for representative samples from each group. Data are presented as the means ± SEM. *P<0.05, **P<0.01, ***P<0.001 vs. WT; $^{\#}$P<0.05, $^{\#\#}$P<0.01, $^{\#\#\#}$P<0.01 vs. eGFP control (CUMS+ AAV-eGFP) by ANOVA with Tukey post hoc correction. WT, wide type.

Supplemental Table 1. PCR primers used in this study

Gene	*Forword (5'→3')*	*Reverse (5'→3')*
BDNF	AATAATGTCTGACCCCAGTGC	GTCACATTGTTGTCACGCTCC
CREB	GCAGTGACTGAGGAGCTTGT	ACTCTGCTGGTTGTCTGCTC
SYN	GTGTGGCTTAAACACAGCGG	TGCACCCTCTCAAACTCCAC
PSD-95	GTTGCAGGTGAATGGAACAGAG	CCTCCCGAACATCCACTTCAT
Bcl-2	GGA TCC AGG ATA ACG GAG GC	ATG CAC CCA GAG TGA TGC AG
Bax	TCT TCA AAC TGC TGG GCC ATT	CTT GTC ACC TGC CTG ACT GCT
Caspase3	GGA GCT TGG AAC GCG AAG AA	ACA CAA GCC CAT TTC AGG GT
Caspase9	CAA GAA GAG CGG TTC CTG GT	CAG AAA CAG CAT TGG CGA CC
GAPDH	AGT GCC AGC CTC GTC TCA TA	GGT AAC CAG GCG TCC GAT AC

KEY RESOURCES TABLE

REAGENT or RESOURCE	SOURCE	IDENTIFIER
Antibodies		
Rabbit polyclonal anti-cleaved Caspase-3	Cell Signaling Technology	Cat#9661; RRID:AB_2341188
Rabbit monoclonal anti-BCL-2	Cell Signaling Technology	Cat#2870; RRID:AB_2290370
Rabbit monoclonal anti-LC3A/B	Cell Signaling Technology	Cat#12741; RRID:AB_2617131
Rabbit monoclonal anti-Beclin-1	Cell Signaling Technology	Cat#3495; RRID:AB_1903911
Rabbit monoclonal anti-PARP	Cell Signaling Technology	Cat#9532; RRID:AB_659884
Rabbit monoclonal anti-PSD-95	Cell Signaling Technology	Cat#3450; RRID:AB_2292883
Rabbit monoclonal anti-β-actin	Cell Signaling Technology	Cat#4970; RRID:AB_2223172
Rabbit monoclonal anti-Synaptophysin	Cell Signaling Technology	Cat#5461; RRID:AB_10698743
Rabbit monoclonal anti-CREB	Cell Signaling Technology	Cat#9197; RRID:AB_331277
Rabbit monoclonal anti-SQSTM1/p62	Cell Signaling Technology	Cat#23214; RRID:AB_2798858
Rabbit polyclonal anti-Phospho-Akt	Cell Signaling Technology	Cat#9271; RRID:AB_329825
Rabbit polyclonal anti-Phospho-p53	Cell Signaling Technology	Cat#9284; RRID:AB_331464
Rabbit polyclonal anti-PI3K	Cell Signaling Technology	Cat#4292; RRID:AB_329869

Rabbit polyclonal anti-PTEN	Cell Signaling Technology	Cat#9552; RRID:AB_10694066
Rabbit monoclonal anti- Synaptotagmin-1	Cell Signaling Technology	Cat#14558; RRID:AB_2798510
Mouse monoclonal Anti-Neuroligin 1	Abcam	Cat# ab186279; RRID:AB_2801327
Rabbit polyclonal anti-BDNF	SANTA	Cat# sc-546; RRID:AB_630940
Rabbit polyclonal anti-GAPDH	Proteintech Group	Cat#10494-1-AP; RRID: AB_2263076
Rabbit polyclonal anti-BAX	Proteintech Group	Cat#50599-2-lg; RRID:AB_2061561
Rabbit polyclonal anti-Caspase9	Bioworld	Cat# AP0359
Goat polyclonal anti-Nestin	Thermofish	Cat# PA5-47378 RRID:AB_2609217
Rabbit polyclonal anti-PSD95	Proteintech Group	Cat# 20665-1-AP
Rabbit monoclonal Synaptophysin	Cell Signaling Technology	Cat# 9020
Rabbit polyclonal anti-Doublecortin（DCX）	Cell Signaling Technology	Cat# 4604
Rabbit polyclonal anti-MAP2	Cell Signaling Technology	Cat# 4542
DAPI	Beyotime Biotechnology	Cat# C1002
Rhodamine (TRITC)-conjugated Donkey anti-Goat IgG	Thermofish	Cat# A-11058 RRID: AB_2534105
Rhodamine (TRITC)-conjugated Goat anti-Rabbit IgG	Proteintech Group	Cat# SA00013-4;
Fluorescein (FITC)-conjugated Goat anti-Mouse IgG	Proteintech Group	Cat# SA00013-1;

Peroxidase-conjugated goat anti-rabbit IgG	Zhongshan Golden Bridge Biotechnology	Cat#ZB-2301; RRID: AB_2747412
Peroxidase-conjugated goat anti-mouse IgG	Zhongshan Golden Bridge Biotechnology	Cat#ZB-2305; RRID: AB_2747415
Chemicals, Peptides, and Recombinant Proteins		
AAV9-rno-mir-26a(43063-1)	Shanghai Genechem	N/A
AAV9-rno-miR-26a-3p-sponge (43023-1)	Shanghai Genechem	N/A
lipopolysaccharide (LPS)	Sigma-Aldrich	Cat# L2880
Hoechst 33258	Solarbio Biotechnology	Cat#C0031
TRIzol	Invitrogen	Cat#15596018
Critical Commercial Assays		
FD Rapid GolgiStain™ Kit	FD Neuro-Technologies	Cat# PK401A
BeyoECL Plus (Ultra sensitive ECL chemiluminescence kit)	Beyotime	Cat# No.P0018S
Immobilon Western (Chemiluminescent HRP Substrate)	MILLIPORE	Cat# No.WBKLS0050
Experimental Models: Organisms/Strains		
Wistar rat	Shandong University Experimental Animal Centre	Custom developed
Oligonucleotides		
Primers for BAX, BCL-2, Caspase 9, Caspase 3, PSD-95, CREB, BDNF, SYN, GAPDH, see Supplemental Table 1	This paper	N/A
Software and Algorithms		

ZEN lite	Carl Zeiss	https://www.zeiss.com/microscopy/int/downloads.html?vaURL=www.zeiss.com/microscopy/int/downloads/zen.html
ImageJ	NIH IMAGEJ	https://imagej.nih.gov/ij/
Graphpad prism 8	Graphpad prism	https://www.graphpad.com/scientific-software/prism/
Photoshop CC	Adobe	https://www.adobe.com/products/photoshop.html